Earth and Planetary Science Letters 408 (2014) 390–401

Contents lists available at ScienceDirect

Earth and Planetary Science Letters

www.elsevier.com/locate/epsl

Temporal variations in the influence of the subducting slab on Central Andean arc magmas: Evidence from boron isotope systematics

Rosemary E. Jones [a,*], Jan C.M. De Hoog [a], Linda A. Kirstein [a], Simone A. Kasemann [b], Richard Hinton [a], Tim Elliott [c], Vanesa D. Litvak [d], EIMF [e]

[a] School of GeoSciences, University of Edinburgh, Grant Institute, West Mains Road, Edinburgh, EH9 3JW, UK
[b] Department of Geosciences & MARUM, Centre for Marine Environmental Sciences, University of Bremen, 28334 Bremen, Germany
[c] School of Earth Sciences, University of Bristol, Wills Memorial Building, Queens Road, Bristol, BS8 1RJ, UK
[d] Instituto de Estudios Andinos Don Pablo Groeber, Departamento de Ciencias Geológicas, Universidad de Buenos Aires – CONICET, Argentina
[e] Edinburgh Ion Microprobe Facility, School of GeoSciences, University of Edinburgh, West Mains Road, Edinburgh, EH9 3JW, UK

ARTICLE INFO

Article history:
Received 17 April 2014
Received in revised form 29 September 2014
Accepted 3 October 2014
Available online 6 November 2014
Editor: B. Marty

Keywords:
boron isotopes
melt inclusions
subduction zone geometry
southern Central Andes
slab-derived fluids
Cenozoic arc magmatism

ABSTRACT

The Pampean flat-slab segment in the southern Central Andes represents an ideal setting at which to investigate how changes in the tectonic configuration of a subduction zone (convergence angles and rates, seamount subduction and shallowing slab angle) affects the recycling of subducted components to arc magmas. To constrain sources, particularly of slab-derived fluids and their contribution to arc magmatism, boron isotope and select major and trace element compositions were determined for pyroxene- and zircon-hosted melt inclusions obtained from a suite of Paleocene to Miocene arc magmatic rocks, from the southern Central Andes. Considerable changes in δ^{11}B values and boron concentrations are observed with time. Significantly lower δ^{11}B values (average $= -1.9 \pm 2.2$‰ (1σ)) and B/Nb ratios (average $= 3.3 \pm 1.3$ (1σ)) were obtained for melt inclusions from Oligocene arc rocks ($\sim$ 24 Ma) compared to those from the Paleocene ($\sim$ 61 Ma) (averages $= +1.6 \pm 0.8$‰ and 17.8 ± 1.4 (1σ), respectively) and the Miocene ($\sim$18 Ma) (averages $= +4.7 \pm 1.9$‰ and 11.9 ± 5.5 (1σ), respectively).
A slab-derived fluid with a δ^{11}B composition of +1.5‰, primarily derived from altered oceanic crust on the down-going slab, affected the source of the Paleocene arc magma. The source of the Oligocene arc magmas received less boron derived from the subducting slab ($\lesssim$1% fluid addition) than the Paleocene and Miocene arc magmas (up to 3.5% fluid addition). This is consistent with a greater depth to the slab-mantle interface and is potentially related to the widening of the volcanic arc and more distal position of these samples relative to the trench during this time period. The higher δ^{11}B values (up to $\sim$9‰) obtained for the Miocene melt inclusions record an increase in the influence of serpentinite-derived fluids on the source of arc magmas after $\sim$19.5 Ma. This is approximately coeval with the subduction of the Juan Fernandez Ridge (JFR), suggesting that the oceanic lithosphere associated with the subducting JFR in the Early Miocene was hydrated and serpentinised, similar to the present day ridge. As serpentinisation increases the buoyancy of the slab this finding supports the link between the intersection of the JFR with the Andean margin and the onset of flat-slab subduction.

1. Introduction

Convergent margins with shallow subducting angles (i.e., <10° at ca. 100 km depth), often referred to as 'flat-slab zones', are frequently linked with an absence of active arc volcanism (Gutscher et al., 2000). Variations in the subduction angle of the Nazca plate beneath the South American continent has resulted in the segmentation of the Andean margin into volcanically active and inactive zones (e.g., Jordán et al., 1983). The southern Central Andes (Pampean flat-slab segment) represent a region which is currently volcanically inactive. Over the latter part of the Cenozoic the angle at which the oceanic plate subducts beneath this section of the Andean margin has shallowed, although the exact timing and cause is debated. Several mechanisms have been proposed, including; (1) the intersection of the Juan Fernandez Ridge (JFR), an intraplate volcanic seamount chain, which began intersecting the Andean margin during the Early Miocene (Gutscher et al., 2000; Pilger, 1981; Yañez et al., 2002, 2001); (2) the curvature of the subducting

* Corresponding author.
E-mail address: r.e.jones001@gmail.com (R.E. Jones).

http://dx.doi.org/10.1016/j.epsl.2014.10.004

slab (Cahill and Isacks, 1992); and (3) the trench-ward motion of the thickened Andean lithosphere (Manea et al., 2012).

The intersection of the JFR with the Central Andean margin coincides with the location of the current flat-slab segment (Anderson et al., 2007). The JFR originates from a narrow mantle plume and is suggested to have begun intersecting the Andean margin at ~20 Ma, migrating south along the margin at a rate of ~200 km/Ma to its current position at 32.5°S (Yañez et al., 2002). Geophysical evidence suggests the current oceanic lithosphere associated with the JFR has been strongly hydrated and serpentinised (Kopp et al., 2004; Marot et al., 2013). Serpentinisation of the oceanic mantle lithosphere is an important mechanism for generating increased buoyancy in the subducting plate and hence can account for the development of flat-slab subduction (Kopp et al., 2004). Whether the oceanic lithosphere associated with the JFR has always been serpentinised, and whether this caused the development of flat-slab subduction in the southern Central Andes during the Early Miocene remains unclear.

In this study we address these outstanding uncertainties by using specific geochemical tracers present in arc magmatic rocks (boron concentrations and isotope ratios) to identify the subduction and dehydration of serpentinite at sub-arc depths. In addition we examine how the contributions of other slab components (altered oceanic crust (AOC), oceanic and continentally derived sediments) to the source of arc magmas have changed with the altering geodynamic setting.

Boron (B) concentrations and isotope ratios have been identified as sensitive indicators of subducting slab components in arc magmatic rocks (e.g., Palmer, 1991; Rosner et al., 2003; Tonarini et al., 2011). Volcanic rocks from both island and continental arcs have much higher B concentrations than MORB, and high ratios of B over incompatible, fluid-immobile elements (e.g., B/Nb, B/Zr), compared to other tectonic settings (e.g., intra-plate volcanism; Ryan et al., 1996). The high concentration of B in comparison to other incompatible, but fluid-immobile elements suggest that the B must be derived from fluids released from the subducting slab, rather than resulting from partial melting or fractional crystallisation. Generally positive δ^{11}B values have been reported for volcanic arc rocks, for example from the Izu (Straub and Layne, 2002), Kurile (Ishikawa and Tera, 1997), Lesser Antilles (Smith et al., 1997), Mariana (Ishikawa and Tera, 1999), South Sandwich (Tonarini et al., 2011) and Kamchatka (Ishikawa et al., 2001) arcs, with a decrease in B concentrations and δ^{11}B values observed from the arc front to the back-arc (e.g., Ishikawa and Tera, 1997; Leeman et al., 2004; Rosner et al., 2003; Ryan et al., 1995) reflecting the decrease in fluid flux during increased subduction of the slab and the preferential release of ^{11}B to slab derived fluids.

Here we present boron isotope and select major and trace element compositions of pyroxene- and zircon-hosted melt inclusions for Cenozoic arc magmatic rocks from the southern Central Andes. Melt inclusions were analysed as they are protected by the surrounding host phenocryst phase from the effects of post depositional alteration, such as hydrothermal alteration (common at this locality; e.g., Bissig et al., 2001), as well as from late stage processes occurring in the melt during magma ascent (e.g., Schiano, 2003; Schmitt et al., 2002; Sobolev, 1996). The obtained melt inclusion data is combined with U–Pb and Ar–Ar ages (Jones, 2014) to constrain changes in the influence of the subducting slab on the source of southern Central Andean arc magmas with time, and to evaluate the potential causes of flat-slab subduction.

2. Geological setting

The study area is located between 29.5 and 31°S in the Pampean flat-slab segment of the southern Central Andes and spans the Principal and Frontal Cordillera of Chile and Argentina (Fig. 1). Subduction of oceanic crust beneath the South American plate has been active since the Jurassic and has produced a series of volcanic arcs (e.g., Charrier et al., 2007; Ramos et al., 2002; Stern, 2004). Convergence rates and the relative plate motions between the oceanic (Farallon and Nazca) and South American plates have changed over time (Somoza and Ghidella, 2012) (Fig. 2). Convergence rates between the oceanic Farallon and the South American plate are thought to have been relatively slow during the Paleocene (~5 cm/yr), with an increase in the Mid Eocene to rates of ~8 cm/yr (Somoza and Ghidella, 2012). This convergence rate is suggested to have remained fairly constant between the Mid Eocene and Late Oligocene, with the Farallon plate being subducted in a north-easterly (NE) direction (Pardo Casas and Molnar, 1987; Pilger, 1984; Somoza and Ghidella, 2012) (Fig. 2). The oceanic lithosphere being subducted during this time interval was most likely Late Cretaceous in age (Somoza and Ghidella, 2012) and subducting at a normal angle (>30°) (Ramos and Folguera, 2009).

A significant change in the tectonic configuration of the Andean margin occurred during the Late Oligocene (~ 25 Ma) due to the break-up of the Farallon plate into the Nazca and Cocos plates (Lonsdale, 2005). This resulted in both an increase in convergence rates (up to ~15 cm/yr) and a change in convergence direction from oblique (NE-SW) to orthogonal (ENE-WSW) (Pardo Casas and Molnar, 1987; Somoza, 1998) (Fig. 2). The westward migration of the South American plate is also thought to have been initiated after ~30 Ma (Silver et al., 1998). This reconfiguration has been linked to a period of major uplift, increased magmatic activity, and a broadening of the magmatic arc (Pilger, 1984). The high convergence rates were sustained up until ~ 20 Ma, and followed by a gradual decline to present day values (~7 cm/yr) (Pilger, 1984; Somoza and Ghidella, 2012). It is suggested that progressively older, Late Cretaceous oceanic lithosphere, originating from the Farallon-Phoenix spreading ridge, was subducted along the South American margin between ~24 and ~16 Ma (Somoza and Ghidella, 2012).

Shallowing of the Nazca plate in the southern Central Andes (~28–33°S) to an angle of ~10° at ~100 km depth is suggested to have been initiated ~18 Ma, as inferred from; (1) the initiation of high angle thrust faulting in the main Andean Cordillera (Maksaev et al., 1984); (2) the broadening of the magmatic arc to the east (Kay and Abbruzzi, 1996; Kay et al., 1987, 1991); (3) the termination of back-arc volcanism (Kay and Mpodozis, 2002); and (4) the initiation of deformation in the Argentinean Precordillera (Jordan et al., 1993). The shallowing of the subducting slab over the latter part of the Miocene caused the migration and expansion of the volcanic arc to the east and the eventual cessation of arc volcanism in the Late Miocene (~6 Ma) (Kay et al., 1987; Ramos et al., 1989; Trumbull et al., 2006). Hence the temporal and spatial distribution of arc volcanism tracks the changing angle of subduction during this time period.

3. Sample selection

Samples of Cenozoic arc magmatic rocks were collected from the Principal and Frontal Cordillera of Chile and Argentina between 29.5 and 31°S (Fig. 1). A subset of eight samples (Table 1) were selected from a larger suite of samples previously characterised and age dated (Jones, 2014). The selection of samples for melt inclusion analysis was based on a number of criteria; (1) in order to assess contributions from slab-derived fluids to the source of the arc magmas and limit the effects of crustal contamination the least evolved samples available were selected; (2) from the most mafic samples those containing suitable melt inclusions for analysis, in suitable phenocryst phases, were selected; (3) finally samples were selected in order to cover the time frame of interest (Paleocene–Miocene). Cenozoic plutonic and volcanic rocks in the

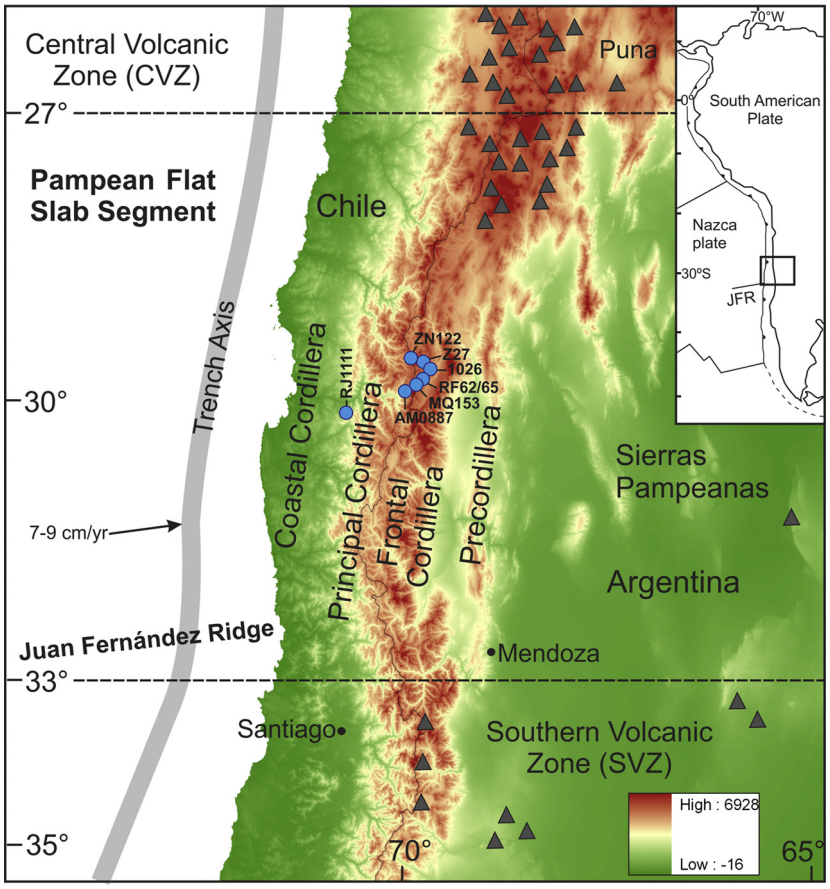

Fig. 1. Map of the study area showing the main features of the present day southern Central Andean margin. Sample locations are shown as blue circles alongside the corresponding sample number. The primary, current active volcanoes are shown as grey triangles. Digital elevation data is from Jarvis et al. (2008). (For interpretation of the references to color in this figure legend, the reader is referred to the web version of this article.)

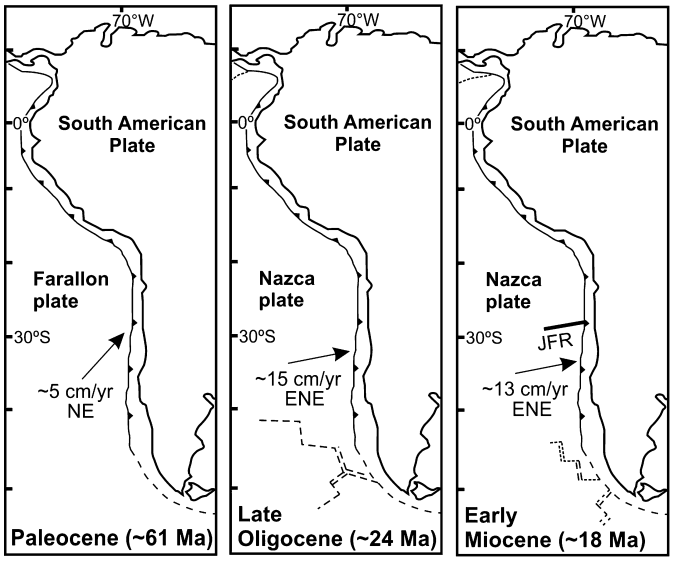

Fig. 2. Relative plate motions between the subducting oceanic plates (Farallon and Nazca) and the South American plate during the three time intervals of interest. References are outlined in the text.

Central Andes are typically highly differentiated so suitable samples available for this kind of study are limited.

The selected samples are extrusive, ranging in composition from basaltic andesites to dacites (54–67 wt% SiO_2) and have medium- to high-K, calk–alkaline compositions (Table 1). The samples with basaltic–andesite, andesite and trachy–andesite compositions contain major phenocryst phases of plagioclase + augite ± enstatite and accessory opaques ± zircon ± apatite. The dacitic sample contains major phenocryst phases of plagioclase + biotite + amphibole and accessory zircon, apatite and opaque phases. The eight samples were age dated prior to this study, either by U–Pb dating of zircon or Ar/Ar dating of plagioclase feldspar (Jones, 2014), and can be divided into three main timeframes: the Paleocene (61.2 ± 1.0 Ma), the Late Oligocene (25.2 ± 0.3 to 23.2 ± 0.3 Ma), and the Miocene (19.3 ± 0.3 to 17.1 ± 0.6 Ma) (Table 1). These ages represent three time periods when the tectonic configuration of the southern Central Andean margin varied (slow, oblique convergence (Paleocene); fast, orthogonal convergence (Late Oligocene); and the initiation of flat-slab subduction (Miocene)). Therefore these samples have the potential to reveal how changes in the configuration of the southern Central Andean subduction zone has affected the recycling of subducted components to arc magmas.

Full details of the sample preparation, analytical methods and data processing can be found in the Supplementary Material.

4. Results

Full results are presented in Table A6, Supplementary Material. Boron concentrations obtained from pyroxene and zircon hosted melt inclusions range from 9 to 218 ppm and $\delta^{11}B$ values range from $-5.4 \pm 1.6‰$ to $+8.6 \pm 1.2‰$ (Fig. 3). The $\delta^{11}B$ values overlap the range of values previously reported for arc rocks from the Central Andes, whereas the boron concentrations extend to slightly higher values (Rosner et al., 2003; Schmitt et al., 2002; Wittenbrink et al., 2009). Boron concentrations obtained for the pyroxene and zircon phenocrysts range between 0.4 and 2.9 ppm.

Table 1
Sample information, ages and whole rock compositions. Ages have been determined by U–Pb dating of zircon and Ar/Ar dating of plagioclase feldspar (highlighted by *) (Jones, 2014). Sample RF65 is assumed to have the same age as RF62 as they are from the same sample location. Whole rock compositions were determined by XRF analysis (Jones, 2014).

Sample	Latitude (S)	Longitude (W)	Formation	Age (Ma)	$\pm 2\sigma$	Geological Epoch	Rock type	SiO_2 (wt%)	TiO_2 (wt%)	Al_2O_3 (wt%)	Fe_2O_3 (wt%)	MnO (wt%)	MgO (wt%)	CaO (wt%)	Na_2O (wt%)	K_2O (wt%)	P_2O_5 (wt%)	LOI	Total
RJ1111	−30.14294	−70.69167	Los Elquinos Formation	61.2*	1.0	Paleocene	Basaltic-andesite	54.2	0.9	17.0	7.7	0.2	5.1	6.5	3.5	2.1	0.1	2.5	99.7
MQ153	−29.85272	−69.86294	Tilito Formation (Lower Doña Ana Group)	25.2	0.3	Oligocene	Andesite	–	–	–	–	–	–	–	–	–	–	–	–
ZN122	−29.57619	−69.92303	Tilito Formation (Lower Doña Ana Group)	24.8	0.4	Oligocene	Andesite	60.7	0.7	15.7	6.4	0.1	3.1	5.9	2.4	2.0	0.2	2.7	99.8
Z27	−29.61389	−69.77611	Tilito Formation (Lower Doña Ana Group)	23.2	0.3	Oligocene	Dacite	66.9	0.7	15.8	4.6	0.0	0.2	3.0	3.6	3.9	0.2	0.9	99.9
AM0887	−29.91972	−69.99472	Escabroso Formation (Upper Doña Ana Group)	19.3*	0.3	Miocene	Andesite	61.7	0.8	16.2	5.6	0.1	2.7	5.0	3.6	2.5	0.2	1.4	99.7
1026	−29.69056	−69.69500	Escabroso Formation (Upper Doña Ana Group)	18.2	0.3	Miocene	Andesite	61.4	0.8	16.5	5.9	0.1	2.3	5.2	3.7	3.0	0.2	0.6	99.7
RF62	−29.79403	−69.78217	Cerro de las Tórtolas Formation	17.1	0.6	Miocene	Trachy-andesite	59.5	0.9	17.7	6.1	0.1	1.3	5.5	3.8	2.9	0.2	1.8	99.6
RF65	−29.79403	−69.78217	Cerro de las Tórtolas Formation	17.1	0.6	Miocene	Andesite	58.2	0.9	17.2	6.5	0.1	2.8	6.4	3.5	2.6	0.2	1.3	99.6

No apparent relationship is observed between boron concentrations and $\delta^{11}B$ values (Fig. 3).

Boron isotope values, and boron concentrations in certain samples, are highly variable and exceed analytical uncertainties (Figs. 3 and 4). Some of the apparent intra-sample variations in boron concentrations are attributed to the effects of melt inclusion re-homogenisation (Supplementary Material), but these effects are negated by using trace element ratios (e.g., B/Nb and B/Zr). The observed intra-sample heterogeneity in boron concentrations and $\delta^{11}B$ values may also reflect real variations due to the trapping of different melt compositions by phenocryst phases which crystallised at different times. For example, variations in the trapped melt compositions may be a result of the assimilation of crustal materials during magma ascent and/or the mixing of magmas with different compositions during progressive crystallisation.

4.1. Limited effects of differentiation

There is no observable correlation between boron concentrations, isotope ratios and the degree of magmatic differentiation (Fig. 4), and values obtained for melt inclusions trapped in different mineral phases, from the same sample, lie within analytical uncertainty (Fig. 3 and Table A6, Supplementary Material). This suggests that the phenocryst phases are trapping melts with the same boron concentrations and isotopic compositions, despite the fact that they may have crystallised at different times during magma differentiation. This combined evidence suggests that magma differentiation has a negligible effect on the $^{11}B/^{10}B$ ratios trapped in silicate melt inclusions, in line with other studies (e.g., Ishikawa and Tera, 1997; Ishikawa et al., 2001). On this basis, the boron compositions obtained for zircon-hosted melt inclusions, which are present in two of the more evolved samples, Z27 (dacite) and MQ153 (andesite), are presented and interpreted alongside the data obtained from pyroxene-hosted inclusions.

4.2. Trace element ratios and $\delta^{11}B$ values as a function of age

The most striking feature of the dataset are the variations in trace element ratios and $\delta^{11}B$ values as a function of sample age. There are significant differences in B/Nb and $\delta^{11}B$ values between samples from different time periods (Fig. 5). Boron isotope values obtained for the Paleocene sample (RJ1111 (~61 Ma)) range between $+0.7 \pm 0.9$‰ and $+3.7 \pm 1.2$‰ and are accompanied by relatively high B/Nb ratios of between 15.6 and 20.7. Melt inclusions from the Late Oligocene samples (~25–23 Ma) show generally negative $\delta^{11}B$ values between -5.4 ± 1.6‰ and $+0.9 \pm 1.7$‰ and low, tightly grouped B/Nb ratios of between 1.5 and 5.7. Boron isotope values obtained for melt inclusions from the Miocene samples (~19–17 Ma) are positive and range between $+0.6 \pm 1.0$‰ and $+8.6 \pm 1.2$‰, with B/Nb ratios ranging from 4.4 to 36.3 (Fig. 5).

5. Discussion

The large, time-dependent range in boron isotopic compositions obtained for the southern Central Andean arc magmas suggests temporal changes in the sourcing of boron, which can be explained by the following scenarios: (1) the melt source regions were affected by fluids derived from different sources; (2) the melt source region received less fluids derived from the subducting slab due to the slab being at greater depth beneath the arc and therefore more dehydrated; and/or (3) the ascending arc magmas assimilated different volumes of Andean continental crust. These scenarios will be evaluated based on boron isotope and trace element systematics of the melt inclusions within the framework of concurrent temporal changes in subduction parameters of the Andean margin during the Cenozoic.

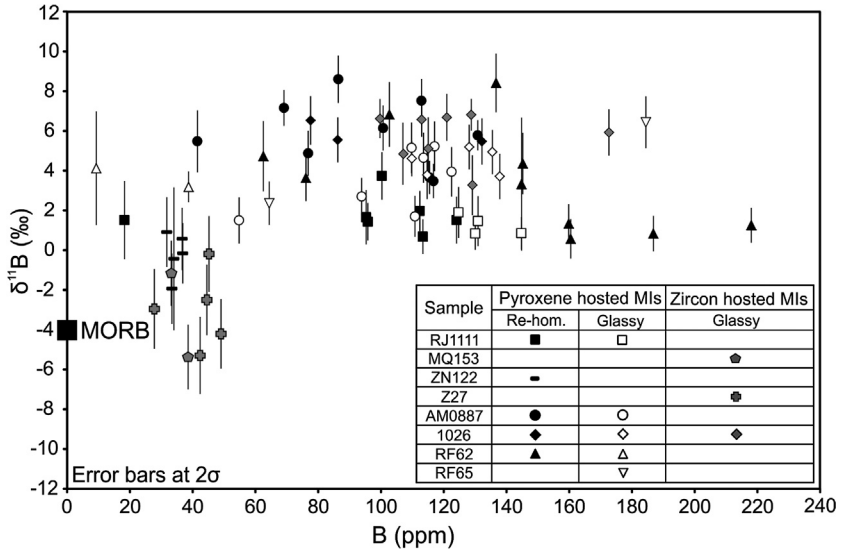

Fig. 3. Boron concentrations (ppm) plotted against δ^{11}B (‰) obtained for pyroxene- and zircon-hosted melt inclusions (MI). Error bars on the δ^{11}B values represent propagated analytical uncertainties at the 2σ level. Errors bars on the boron concentrations are smaller than the symbol size.

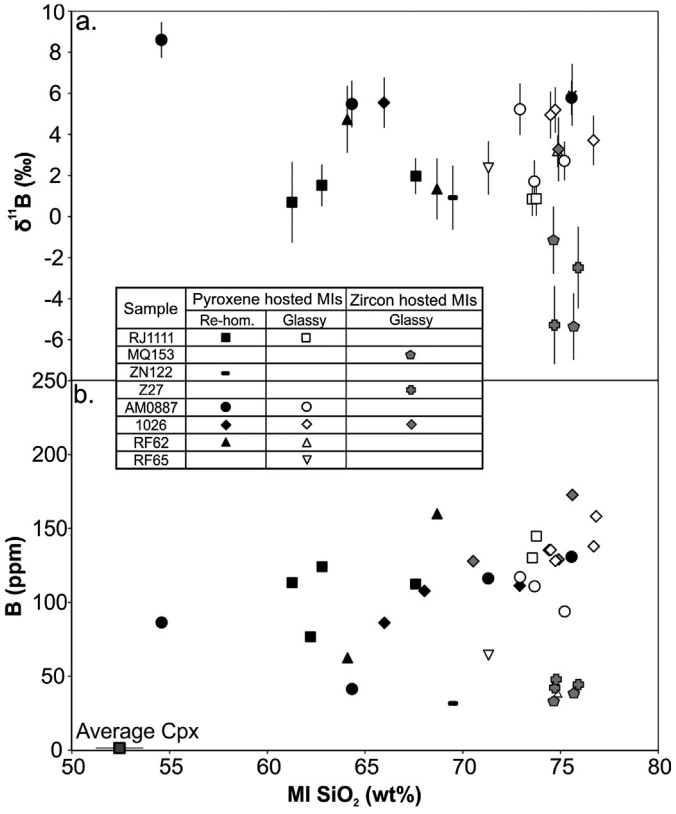

Fig. 4. Boron isotope values (‰) and B concentrations (ppm) plotted against SiO_2 (wt%) contents for pyroxene- and zircon-hosted melt inclusions. Error bars on the δ^{11}B values represent propagated analytical uncertainties at the 2σ level. Errors bars on the boron concentrations are smaller than the symbol size.

5.1. Potential sources of boron in southern Central Andean arc magmas

Boron sources which may contribute to arc magmas include the depleted mantle wedge, serpentinised peridotite from oceanic lithosphere or mantle wedge, altered oceanic crust (AOC), subducted sediments, and the continental crust, all of which have varied boron contents and boron isotope compositions. The Andean mantle wedge is considered to have a similar composition to that of MORB-source mantle (Lucassen et al., 2002) which has very low boron concentrations of $\sim$0.05 ppm with a δ^{11}B value of -4.0‰ (Chaussidon and Marty, 1995). Therefore melting of the mantle wedge contributes negligible boron to primary arc magmas and has little impact upon their δ^{11}B compositions.

Crustal contamination and assimilation processes have previously been invoked in the petrogenesis of Central Andean arc magmas (e.g., Davidson and de Silva, 1992; Hildreth and Moorbath, 1988; James, 1982). Oxygen and hafnium isotopic signatures obtained for zircons present in Late Oligocene–Miocene arc samples from the Pampean flat-slab segment, along with the presence of inherited zircon cores, suggests that some of the arc magmas have been contaminated via assimilation of the Late Palaeozoic–Early Mesozoic basement (Jones, 2014). An average boron concentration of 43 ppm and a δ^{11}B value of -8.9 ± 2.3‰ has been reported for the Palaeozoic and Mesozoic Central Andean basement (Kasemann et al., 2000), which overlaps with the estimated average range of global continental crust (-8 to -13‰; Chaussidon and Albaréde, 1992). Consequently, crustal contamination of mantle-derived arc magmas would lead to comparably negative boron isotope compositions, relative to the mantle.

Mafic portions of the oceanic crust have low B contents when formed, but due to hydrothermal interaction with seawater ($\sim$4.5 ppm B with $\delta^{11}B = +39.5$‰; Spivack and Edmond, 1987), altered oceanic crust has considerably higher B concentrations (>1 to 69 ppm) and δ^{11}B values ($\sim$0 to +9‰) (Smith et al., 1995; Spivack and Edmond, 1987; Yamaoka et al., 2011, 2012). Progressive metamorphic devolitisation of the oceanic crust during subduction releases boron, and preferentially ^{11}B, into slab-derived fluids (King et al., 2007; Moran et al., 1992; Peacock and Hervig, 1999). Therefore fluids released from the slab become isotopically lighter and contain less boron as the oceanic crust is subducted to greater depths.

Subducting sediments have highly variable boron concentrations and isotope ratios (Ishikawa and Nakamura, 1993), reflecting variable proportions of continental detritus with negative δ^{11}B values (30 $->$100 ppm B and $\delta^{11}B = -8$ to -13‰), and pelagic sediments with positive δ^{11}B values (1–150 ppm B and $\delta^{11}B = +2.1$ to +26.2‰). The composition and quantity of the sediment entering the sub arc region in the southern Central Andes is difficult to estimate and is likely to have changed over the course of the Cenozoic due to a wide range of factors including climate, productivity, erosion rates, sediment routing and levels of sediment accretion. The Central Andean margin is currently non-accretionary

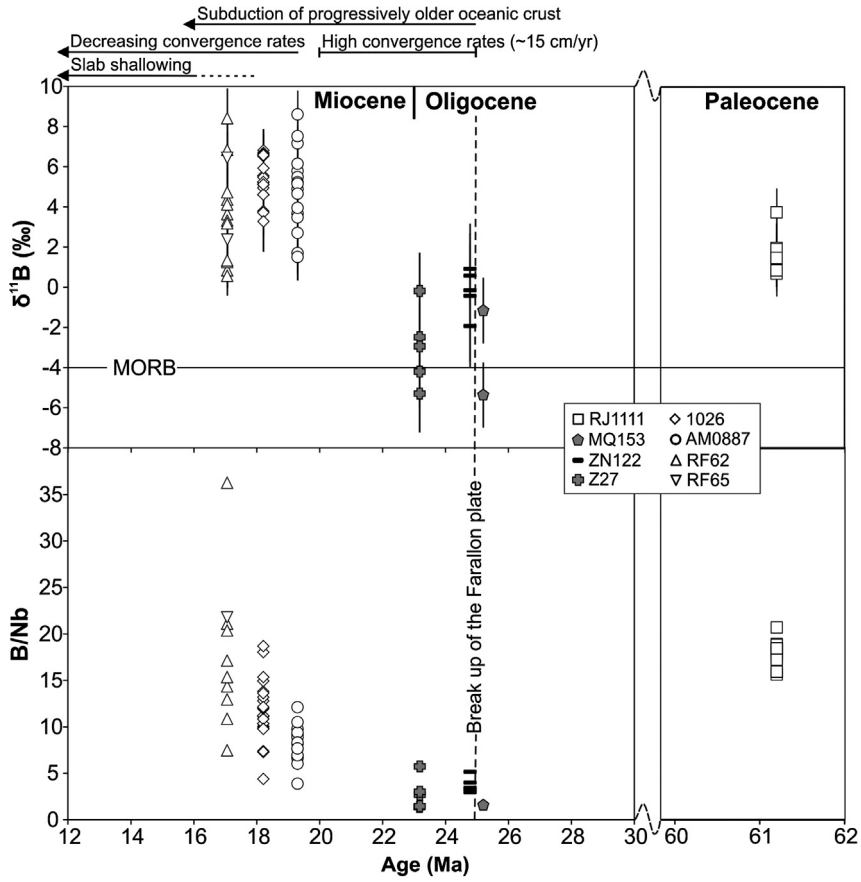

Fig. 5. Boron isotope values (‰) and B/Nb ratios plotted against sample age. Key tectonic events, changes in convergence rates and the δ^{11}B value for MORB are highlighted (refer to text for references). MORB has a B/Nb ratio of 0.3 (Chaussidon and Marty, 1995; Workman and Hart, 2005). Error bars on the δ^{11}B values represent propagated uncertainties at the 2σ level.

(Von Huene and Scholl, 1991) and high levels of subduction erosion have been proposed for the Cenozoic (e.g., Goss et al., 2013; Kay et al., 2005; Rutland, 1971; Stern, 1991). It is suggested that the majority of sediment currently present in the Chile trench is derived from the South American continent (Kilian and Behrmann, 2003; Scholl et al., 1970; Thornburg and Kulm, 1987a, 1987b). Therefore the subducting sediments are likely to have a negative boron isotope value reflecting that of the Central Andean basement (-8.9 ± 2.3‰; Kasemann et al., 2000) and continental detritus (-8 to -13‰; Ishikawa and Nakamura, 1993).

A final potential source of B in subduction zones is serpentinised peridotite, either in the oceanic crust (abyssal peridotites), the ocean lithospheric mantle, or the mantle wedge. As serpentinite can contain >13 wt% H_2O, its breakdown has the potential to release large quantities of water into the mantle wedge (e.g., Rüpke et al., 2004; Spandler and Pirard, 2013). The breakdown of serpentinite mineral phases into forsterite and enstatite occurs at temperatures of ~650 °C (Ulmer and Trommsdorff, 1995; Wunder et al., 2001), which in the majority of subduction zones corresponds to depths beneath or behind the arc (e.g., Syracuse et al., 2010). During serpentinisation, boron and preferentially ^{11}B is added to peridotite, resulting in positive δ^{11}B values (δ^{11}B = +8.3 to +12.6‰) and high boron concentrations (50–81 ppm) (Spivack and Edmond, 1987). Even heavier δ^{11}B values ranging between +29.6 and +40.5‰ have been reported for highly serpentinised, spinel harzburgites from the Mid-Atlantic ridge (Vils et al., 2009). The degree of hydration and serpentinisation of the oceanic lithosphere is influenced by the rate of seafloor spreading; at slow spreading centres this process is thought to be more significant than at fast spreading centres (Escartín et al., 1997; Francis, 1981; Iyer et al., 2010). Transform faults (e.g., Hekinian et al., 1992; Melson and Thompson, 1971), faulting associated with the development of seamount chains (e.g., Kopp et al., 2004), and deep normal faulting of the outer rise before the oceanic plate enters the trench (e.g., Ranero et al., 2003; Ranero and Sallarès, 2004) are important pathways for hydrating and serpentinising the oceanic lithosphere away from spreading centres.

The boron composition of serpentinites present in the oceanic lithosphere are also likely to change with depth, depending on the temperature and pH conditions. Due to low temperature (<200 °C) interaction with seawater, serpentinites formed close to the surface of the oceanic crust are likely to have seawater-like δ^{11}B values (δ^{11}B = +40‰). The circulation of high-temperature (ca. 350 °C) hydrothermal fluids has been shown to result in serpentinites with lower δ^{11}B values at deeper levels in the oceanic crust. However, these values are still relatively high, with δ^{11}B values of between +9 and +20‰ being reported for serpentinites which have been affected by high temperature (300–350 °C), low pH (4–5) hydrothermal fluids circulating at deeper levels in the oceanic crust (Harvey et al., 2014).

5.2. Source variations with time

In order to quantify the contribution of different potential sources to the composition of southern Central Andean arc magmas, multi-component mixing models have been generated following the methods of Marschall et al. (2008) and Tonarini et al. (2011). The δ^{11}B and Nb/B values obtained for the Paleocene, Oligocene and Miocene samples are used to estimate levels of boron and hence fluid addition from different sources. Two major reservoirs are considered: the uppermost slab, which is

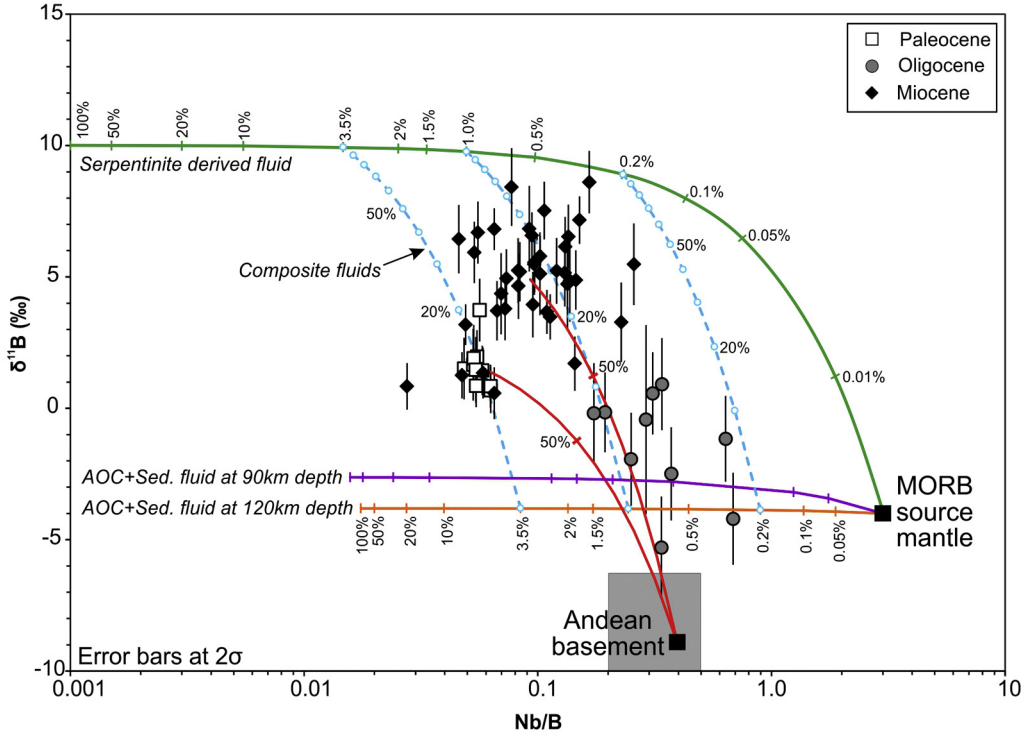

Fig. 6. Plot of Nb/B ratios versus δ^{11}B values for melt inclusions from Paleocene, Oligocene and Miocene arc rock samples. Mixing lines are shown for the addition of fluids derived from dehydrating serpentinite to the mantle wedge (MORB source mantle; Chaussidon and Marty, 1995; Workman and Hart, 2005), and fluids derived from AOC + sediments at different depths to the top of the slab (90 and 120 km). The numbers indicate the amount of fluid added to the mantle wedge as a percentage and the values used in the model are presented in Table 2. A ratio of 90:10 is assumed for AOC and sediment. Bulk mixing lines between the average compositions for the Paleocene and Miocene samples and the average Andean crust (Kasemann et al., 2000) and composite fluid mixing lines (dashed) are also shown.

Table 2
Parameters used in mixing models. Data sources: a. Chaussidon and Marty (1995); b. Workman and Hart (2005); c. this study; d. Spivack and Edmond (1987); e. following the method of Tonarini et al. (2011); f. Kasemann et al. (2000); and g. Jones (2014).

	δ^{11}B (‰)		B (ppm)		Nb/B	
MORB source mantle	−4.0	a	0.05	a	3	a, b
AOC + sediment derived fluid at 90 km depth	−2.6	c	71	c	0.016	c
AOC + sediment derived fluid at 120 km depth	−3.8	c	60	c	0.018	c
Serpentinite derived fluid	10	d	300	c	0.001	e
Andean basement	−8.9	f	43	f	0.4	f, g

represented by a 7 km thick mafic crust and a 1.3 km thick layer of sediments (cf. Syracuse et al., 2010); and the partially serpentinised ultramafic portion of the subducting oceanic lithosphere. In addition to these fluid sources the overlying Andean continental crust is considered as an additional potential boron source. The boron isotopic composition of AOC at 30 km depth is assumed to be −6‰ based on natural samples of the subducting slab recovered from the Mariana fore-arc (Pabst et al., 2012). This value was used to avoid uncertainties involved with shallow fluid release. The δ^{11}B composition used for serpentinite is the +10‰ value reported by Boschi et al. (2008) for abyssal serpentinites. The starting value used for sediment in the model is −8‰ at 20 km depth and evolves to −15‰ at 90–120 km depth due to the preferential release of ^{11}B into slab-derived fluids (cf. Section 5.1). In order to account for the reduction in both δ^{11}B values and the concentrations of boron in slab-derived fluids with progressive heating and dehydration of the slab, dehydration of the subducting slab has been modelled in 10 km intervals starting at 20 km depth using the T550 thermal parameters for the Central Chile arc section (Syracuse et al., 2010) combined with the dehydration depths estimated from van Keken et al. (2011). Sediment dehydration was modelled using slab top temperatures, whereas AOC was modelled using a temperature profile interpolated between slab top and the Moho (Syracuse et al., 2010) in order to reflect the lower temperatures present in the interior of the oceanic crust (Fig. A7, Supplementary Material). Total amounts of fluid released from sediment and AOC are 5.6 wt% and 5 wt% H_2O, respectively (Fig. A8, Supplementary Material). Due to the expulsion of pore waters, low grade metamorphism, and the mobilisation of volatiles from subducting sediments at shallow depths (prior to ∼40 km) (Peacock, 1990; Savov et al., 2007; You et al., 1995, 1996), alongside the hot nature of the Central Andean subduction zone (Syracuse et al., 2010), the subducting sediment has already lost 98% of its associated fluid by the time it reaches 90–120 km depth (i.e., sub-arc depths) (Fig. A8, Supplementary Material). Therefore the composition of the subducting sediment plays a very minor role in modelling the composition of arc magmas.

As opposed to continuous dehydration of AOC and sediment, serpentinite dehydrates at temperatures of ∼650 °C (although some B may be lost during the lizardite–antigorite transition; e.g., Vils et al., 2011), which according to the Central Chile temperature profile occurs right beneath the arc at the top of the ocean mantle lithosphere (Syracuse et al., 2010). As this is the coldest part of the slab, ultramafic portions of the oceanic crust will have released their fluids at shallower depths.

5.2.1. Paleocene; evidence for a homogeneous slab-derived fluid

The δ^{11}B values of melt inclusions from the Paleocene sample (+0.7 to +3.7‰) display little variation compared to individual samples from the Oligocene and Miocene (Fig. 6), suggesting a relatively homogeneous boron source in this instance. The δ^{11}B values are too high to be accounted for by the addition of boron derived from the existing Andean continental crust, for which negative δ^{11}B values have been obtained (Kasemann et al., 2000) (Fig. 6). This is consistent with other lines of evidence which suggest that the Paleocene arc magmatic rocks from the Principal Cordillera of Chile, assimilated very little (<5% bulk) Andean continental crust on route to the surface (e.g., Jones, 2014; Parada et al., 1988). This implies that virtually all the boron present in this sample must be derived from subducting components.

No individual fluid source in our model has a δ^{11}B value similar to that obtained for the Paleocene sample (approximately +1.5‰), as AOC + sediment-derived fluids have δ^{11}B values <0‰ at relevant slab depths (i.e., >90 km), whereas serpentinite-derived fluids have much higher δ^{11}B values (up to +10‰) (Fig. 6). Therefore, the boron-containing fluids affecting the sub-arc mantle are most likely a mixture derived from these different subducting components (serpentinite, AOC and sediments). Our mixing calculations indicate that the addition of ~3.5% fluid to the source of the arc magma with approximately 80–90% derived from AOC (and sediments) and 10–20% derived from dehydrating serpentinite, could account for the boron compositions obtained for the Paleocene sample (Fig. 6).

5.2.2. Oligocene: a broad magmatic arc

Boron isotopic compositions of Oligocene samples of the Tilito Formation (−5.4 to +0.9‰) extend to considerably lower values than those obtained for the Paleocene sample (Fig. 6), indicating an increased contribution of low δ^{11}B sources, e.g., the assimilation of continental crust during magma ascent. The B contents of Oligocene melt inclusions (39 ± 13 ppm B) are very similar to those obtained for the Palaeozoic–Mesozoic Central Andean basement (~43 ppm). However, the δ^{11}B values are slightly heavier (−5.4 to +0.9‰) than the basement (-8.9 ± 2.3‰) (Kasemann et al., 2000). The low boron concentrations (high Nb/B ratios) of most of the Oligocene arc volcanic rocks could potentially be explained by the contamination of arc magmas with Paleozoic–Mesozoic Andean crust. However, if the source of the arc magmas was being influenced by slab-derived fluids with a similar boron composition to those affecting the sub-arc mantle in the Paleocene example, assimilation of very large volumes (>50% bulk assimilation) would be required to explain the majority of the δ^{11}B and Nb/B values (Fig. 6). Thermal limits render that the assimilation of this quantity of felsic crust by mantle-derived melts inconceivable (Reiners et al., 1995). This high degree of crustal contamination is also inconsistent with the levels of crustal assimilation suggested by the oxygen and hafnium isotopic composition of magmatic zircon obtained for these samples (5–15%) (Jones, 2014). These samples lack any evidence for inherited zircon, as demonstrated by consistent U–Pb ages and isotopic compositions, combined with the lack of any apparent xenocrystic zircon cores from cathodoluminescence imaging, which might be expected for volcanic rocks which have assimilated large volumes of older, felsic crust (Jones, 2014). Additionally, no signification correlation is seen between melt inclusion and whole rock SiO_2 contents and δ^{11}B values in these samples (Fig. 4), which might be expected with progressive crustal assimilation. Overall this implies that whilst the progressive assimilation of continental crust could account for some of the intra-sample variation in δ^{11}B values and TE ratios, that the Oligocene arc magmas must have also received contributions of boron from slab-derived fluids, but with a different composition to those influencing the melt source region at ~61 Ma. This could either be a result of a change in the relative proportions, or compositions, of the subducting components and/or a change in the depth to the top of the slab beneath the arc.

The amount of slab-derived fluid added to the source of the Oligocene arc magmas appears reduced ($\lesssim$1% fluid addition) in comparison to the source of the Paleocene arc magma (Fig. 6). This reduction in fluid contribution, as well as the change in the boron composition of the slab-derived fluids, may be related to changes in the configuration of the Andean margin and the volcanic arc during the Late Oligocene. During this time interval (after ~25 Ma) convergence rates between the Nazca and the South American plates increased to a rate of ~15 cm/yr and the angle of convergence became more normal with the Andean margin (Lonsdale, 2005; Pardo Casas and Molnar, 1987; Somoza, 1998; Somoza and Ghidella, 2012). These increased convergence rates are thought to have resulted in thickening of the continental crust in the northern Central Andes (Isacks, 1988; Oncken et al., 2006) but are suggested to have led to a more extensional regime in the southern Central Andes (Jordon et al., 2001). As a result the magmatic arc broadened in the southern Central Andes (Pilger, 1984) and there is coeval back-arc volcanism (Litvak and Poma, 2010; Ramos et al., 1989). This implies that arc magmatism during the Late Oligocene had a wide across-arc extent and is likely to have been emplaced over a wide range of depths to the slab–mantle interface. Several studies have shown that across arc variations in boron abundance and isotopic composition of arc magmas can be related to the depth of the Wadati-Benioff Zone (WBZ), with the heaviest δ^{11}B values and the greatest B enrichment observed in magmatic rocks from the arc front and decreasing values towards the back arc (e.g., Ishikawa and Tera, 1997; Ishikawa et al., 2001; Leeman et al., 2004; Rosner et al., 2003; Ryan et al., 1995). This has been related to the progressive metamorphic devolatisation and the reduction in fluids coming off the slab as it descends into the mantle, alongside the preferential release of ^{11}B over ^{10}B into these slab-derived fluids (King et al., 2007; Peacock and Hervig, 1999).

In the Andean Central Volcanic Zone (22–27°S, i.e. north of the Pampean flat-slab region) boron concentrations and δ^{11}B values decrease with increasing depth to the WBZ (Rosner et al., 2003). δ^{11}B values (−2.1‰ to −7.2‰) and B concentrations (10–20 ppm) were obtained for Quaternary volcanic rocks located in the back arc, where depths to the WBZ range from 123 to 152 km (Cahill and Isacks, 1992). These values are very similar to those obtained for our Oligocene samples. Using the Andean Central Volcanic Zone as a comparable geological setting to the southern Central Andean margin during the Late Oligocene (i.e., prior to slab shallowing), we suggest that the Tilito Formation was emplaced over a greater depth to the WBZ than the Paleocene arc magmatic rocks, and that the lower δ^{11}B and higher B/Nb ratios reflect decreasing fluid flux from the slab with progressive dehydration (Fig. 7). This is consistent with a low fluid contribution ($\lesssim$1%) in the mixing model (Fig. 6). Evidence from whole rock geochemistry also suggests the most eastern extent of the Oligocene Tilito Formation, located in the Frontal Cordillera of Argentina, may have been emplaced in a more extensional setting (Jones, 2014; Winocur et al., 2014). Higher boron concentrations and δ^{11}B values comparable to those from the Paleocene sample may be present in Oligocene arc magmatic rocks closer to the trench, where the depth to the WBZ was shallower. Unfortunately samples from these frontal arc locations did not contain suitable melt inclusions for boron isotope analysis.

Due to the diminished influence of slab-derived fluids on the source of the Oligocene arc magmas (sampled as part of this study), the δ^{11}B compositions of the melt inclusions are therefore more likely to have been more affected by the assimilation

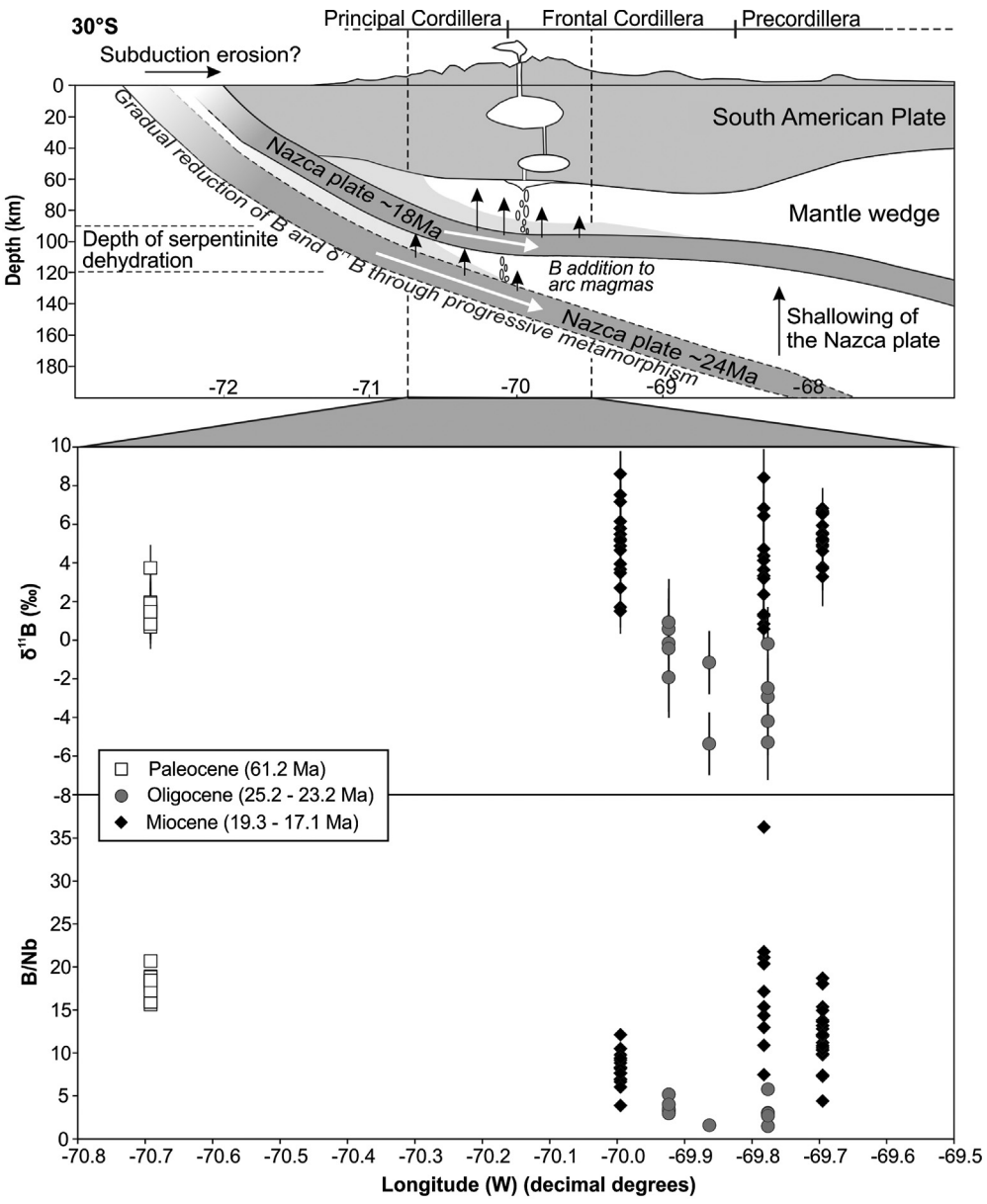

Fig. 7. Boron isotope values and B/Nb ratios plotted against longitude (°W) and displayed against a schematic cross section of the Andean margin at 30°S showing the approximate depths to the subducting Nazca plate below the volcanic arc during the Late Oligocene (~24 Ma) and the Early Miocene (~18 Ma). The depths to the top of the subducting slab for the two different time frames are estimated using the findings of Rosner et al. (2003) (see text for discussion).

of crustal boron than the Miocene arc magmas, which are shown to have received a greater addition of boron from slab-derived fluids (Section 5.2.3).

5.2.3. Miocene: subduction of a seamount chain

Similarly to the values obtained for the Oligocene samples the Nb/B and δ^{11}B values obtained for the Miocene melt inclusions do not define a simple mixing trend and show significant scatter (Fig. 6). Several lines of evidence suggest that these Miocene arc magmas have been affected by crustal contamination during migration through the Andean continental crust (e.g., Jones, 2014; Kay et al., 2005; Litvak et al., 2007). Oxygen and hafnium isotopic variability of zircons from the Miocene samples 1026 and RF62 suggests the mantle-derived melts assimilated between 5 and 15% Palaeozoic–Mesozoic crust on route to the surface, a similar amount to the Oligocene arc magmas (Jones, 2014). Hence, progressive assimilation and/or the assimilation of different amounts of Palaeozoic–Mesozoic basement is suggested to account for some of the observed variability in B composition.

However, the positive δ^{11}B values (average $= +4.7 \pm 1.9$‰) obtained for the melt inclusions from the Miocene samples cannot be accounted for by the assimilation of the Andean continental crust, which has a negative δ^{11}B composition (-8.9 ± 2.3‰; Kasemann et al., 2000). These high δ^{11}B values indicate a greater contribution of fluids derived from dehydrating serpentinite to the melt source region during the Early Miocene, than during the Paleocene (~61 Ma) and Late Oligocene (~24 Ma) (Fig. 6). Serpentinite is the only conceivable source of heavy boron at sub-arc depths, as fluids derived from AOC, combined with subducting sediments, have a maximum δ^{11}B value of -2.6‰ at a depth of 90 km and even lower at greater depths (Fig. 6). The mixing models suggest that on average between 20 and 60% of the fluid affecting the Miocene melt source region is derived from dehydrating serpentinite (Fig. 6).

Serpentinite in subduction zones can be present in the subducting oceanic lithosphere as well as in the mantle wedge due to the serpentinisation of mantle peridotite by fluids released from

the subducting slab at shallow depths beneath the fore-arc (e.g., Hattori and Guillot, 2003; Hyndman and Peacock, 2003; Straub and Layne, 2002; Tonarini et al., 2011). Due to the thermal structure of the Central Andean subduction zone (e.g., Syracuse et al., 2010) it is unlikely that fore-arc mantle wedge serpentinites are retained to sub-arc depths, as temperatures in the mantle wedge well exceed the stability limit of serpentinite (ca. 650 °C; Ulmer and Trommsdorff, 1995). However, the composition and geometry of the subduction interface is complex, with interaction between mafic crust, sediments and mantle wedge peridotite leading to the formation of a highly heterogeneous subduction channel in which hydrous phases such as chlorite can be stable to significantly higher temperatures than serpentine (Marschall and Schumacher, 2012; Ryan and Chauvel, 2014). On the other hand, the thermal gradient observed across the subducting oceanic lithosphere predicts that serpentinites present in the deep oceanic crust and the top of the oceanic mantle lithosphere dehydrate beneath the position of the Central Chilean arc (Syracuse et al., 2010). Therefore, the fluids affecting the source of the Early Miocene arc magmas in the southern Central Andes are suggested to be derived from serpentinised oceanic lithosphere, combined with fluids derived from AOC and sediments, and potentially the subduction channel.

Due to increased relative buoyancy, shallow subduction angles are often linked with the subduction of thickened oceanic lithosphere associated with aseismic ridges, seamount chains and oceanic plateaus (Cross and Pilger, 1982; Gutscher et al., 2000; McGeary et al., 1985; van Hunen et al., 2002). However, only minor thickening of the oceanic crust is associated with the JFR suggesting a limited increase in buoyancy via this process (Kopp et al., 2004). This is insufficient to account for sustained flat-slab subduction more than 700 km beneath the South American continent (van Hunen et al., 2002). Hydration and serpentinisation of mantle peridotite leads a reduction in density from ~3.2 g/cm^3 to ~2.7 g/cm^3 and is combined with an increase in volume of up to 30%. Therefore serpentinisation is an alternate method of generating increased buoyancy in the subducting oceanic plate. Geophysical evidence suggests that the oceanic crust associated with the current JFR is highly faulted and that the oceanic lithosphere has been affected by hydration and mineral alteration, leading to up to ~20% serpentinisation (Kopp et al., 2004). The high δ^{11}B values obtained for the Miocene arc rocks are consistent with a highly serpentinised oceanic lithosphere associated with the subduction of the JFR during the Early Miocene. Consequently, our findings support the link between the subduction of the JFR and the development of flat-slab subduction in the southern Central Andes during the latter part of the Cenozoic.

The lower Nb/B ratios obtained for Miocene samples suggests the source of these arc magmas received a greater addition of slab-derived fluids (up to ~3.5%) compared to the source of the Oligocene arc lavas sampled as part of this study (Fig. 6). This suggests the emplacement of these arc magmas over a less dehydrated slab and therefore a shallower depth to the WBZ (Fig. 7). The combined increase in B concentrations and δ^{11}B values could be interpreted as reflecting the emplacement of the arc magmas over a shallower depth to the slab-mantle interface. In order to generate the values obtained for the Miocene melt inclusions the depth to the WBZ beneath the arc would have to be <60 km (Fig. A9, Supplementary Material). Various lines of evidence have suggested that the initiation of slab shallowing and the associated increase in compression in the overlying Andean crust was not initiated until after 18 Ma (e.g., Jordán et al., 1983; Kay and Abbruzzi, 1996; Kay and Mpodozis, 2002; Maksaev et al., 1984). Therefore, we consider the high B concentrations and δ^{11}B values obtained for the Miocene samples, which range in age between 19.3 and 17.1 Ma, to reflect the initial subduction of the JFR and the associated hydrated and serpentinised lithosphere, rather than a significant shallowing of the slab and decrease in the depth to the WBZ beneath the arc, as this would need time to develop.

6. Conclusions

1. Magma differentiation has a negligible effect on boron concentrations and δ^{11}B values trapped in melt inclusion glasses. Therefore the δ^{11}B values and boron concentrations recorded by melt inclusions present in arc magmatic rocks from the southern Central Andes can be used to assess changes in slab-derived fluids to magma source regions over time.
2. The compositions obtained for melt inclusions from the Paleocene sample suggests the addition of a slab-derived fluid with a relatively homogeneous boron isotopic composition of approximately +1.5‰, to the magma source region at ~61 Ma. This boron isotopic composition suggests that this fluid was likely derived from AOC in the subducting Farallon plate, with a minor component derived from subducting sediments and dehydrating serpentinite.
3. The source of the Oligocene arc magmatic rocks records a diminished influence of slab-derived fluids with more negative δ^{11}B values, compared to the Paleocene and Miocene arc magmatic rocks. This is indicative of a greater depth of the slab-mantle interface due to broadening of the southern Central Andean magmatic arc during this time period.
4. The Miocene samples record the highest δ^{11}B values (+0.8 to +8.6‰) suggesting the source of the arc magmas received a greater contribution from dehydrating serpentinite than those affecting the Paleocene and Oligocene melt source regions. This timing is approximately coeval with the intersection of the JFR with the Andean margin (~20 Ma). It is therefore suggested that similarly to the oceanic lithosphere associated with the present day JFR, the oceanic lithosphere associated with the JFR being subducted during the Early Miocene was also hydrated and serpentinised, hence enhancing the link between the subduction of the JFR and the onset of flat-slab subduction.
5. Some of the intra-sample variations in δ^{11}B and trace element ratios obtained for the Oligocene and Miocene aged samples are likely to reflect the progressive assimilation of the existing Andean continental crust (between ~5–15%) as the arc magmas migrated towards the surface.

Acknowledgements

This work was funded by a NERC CASE studentship (NE/G524128/1) and the Derek and Maureen Moss Scholarship. SIMS analysis at the EIMF was supported by NERC (IMF450/1011). We are grateful to Benjamin Heit, Ricardo Alonso and Dante Scatolon for assistance in fieldwork planning and logistics. Igor Nikogosian and John Craven are thanked for their expertise and assistance in melt inclusion re-homogenisation. We are also grateful to Chris Hayward for support in EPMA, Nicola Cayzer for guidance in SEM imaging, and to Robert McDonald and Mike Hall for advice and assistance with mineral separation and sample preparation. We would like to thank Samuele Agostini, Jeffrey Ryan, Bill Leeman and one anonymous reviewer for their careful and considered reviews which have greatly improved this manuscript.

Appendix A. Supplementary material

Supplementary material related to this article can be found online at http://dx.doi.org/10.1016/j.epsl.2014.10.004.

References

Anderson, M., Alvarado, P., Zandt, G., Beck, S., 2007. Geometry and brittle deformation of the subducting Nazca Plate, Central Chile and Argentina. Geophys. J. Int. 171, 419–434.

Bissig, T., Lee, J.K.W., Clark, A.H., Heather, K.B., 2001. The Cenozoic history of volcanism and hydrothermal alteration in the Central Andean flat-slab region: new ^{40}Ar–^{39}Ar constraints from the El Indio–Pascua Au (–Ag, Cu) belt, 29°20′–30°30′S. Int. Geol. Rev. 43, 312–340.

Boschi, C., Dini, A., Früh-Green, G.L., Kelley, D.S., 2008. Isotopic and element exchange during serpentinization and metasomatism at the Atlantis Massif (MAR 30 N): insights from B and Sr isotope data. Geochim. Cosmochim. Acta 72, 1801–1823.

Cahill, T., Isacks, B.L., 1992. Seismicty and shape of the Subducted Nazca Plate. J. Geophys. Res. 97, 17503–17529.

Charrier, R., Pinto, L., Rodríguez, M.P., 2007. Tectonostratigraphic evolution of the Andean Orogen in Chile. In: Moreno, T., Gibbons, W. (Eds.), The Geology of Chile. The Geological Society, London, pp. 21–114.

Chaussidon, M., Albaréde, F., 1992. Secular boron isotope variations in the continental crust: an ion microprobe study. Earth Planet. Sci. Lett. 108, 229–241.

Chaussidon, M., Marty, B., 1995. Primitive boron isotope composition of the mantle. Science 269, 383–386.

Cross, T.A., Pilger, R.H., 1982. Controls of subduction geometry, location of magmatic arcs, and tectonics of arc and back-arc regions. Geol. Soc. Am. Bull. 93, 545–562.

Davidson, J.P., de Silva, S.L., 1992. Volcanic rocks from the Bolivian Altiplano: insights into crustal structure, contamination, and magma genesis in the central Andes. Geology 20, 1127–1130.

Escartín, J., Hirth, G., Evans, B., 1997. Effects of serpentinization on the lithospheric strength and the style of normal faulting at slow-spreading ridges. Earth Planet. Sci. Lett. 151, 181–189.

Francis, T.J.G., 1981. Serpentinization faults and their role in the tectonics of slow spreading ridges. J. Geophys. Res., Solid Earth 86, 11616–11622.

Goss, A.R., Kay, S.M., Mpodozis, C., 2013. Andean adakite-like high-Mg andesites on the northern margin of the Chilean–Pampean flat-slab (27–28·5°S) associated with frontal arc migration and fore-arc subduction erosion. J. Petrol. 54, 2193–2234.

Gutscher, M.A., Spakman, W., Bijwaard, H., Engdahl, E.R., 2000. Geodynamics of flat subduction: seismicity and tomographic constraints from the Andean margin. Tectonics 19, 814–833.

Harvey, J., Savov, I.P., Agostini, S., Cliff, R.A., Walshaw, R., 2014. Si-metasomatism in serpentinized peridotite: the effects of talc-alteration on strontium and boron isotopes in abyssal serpentinites from Hole 1268a, ODP Leg 209. Geochim. Cosmochim. Acta 126, 30–48.

Hattori, K.H., Guillot, S., 2003. Volcanic fronts form as a consequence of serpentinite dehydration in the forearc mantle wedge. Geology 31, 525–528.

Hekinian, R., Bideau, D., Cannat, M., Francheteau, J., Hébert, R., 1992. Volcanic activity and crust-mantle exposure in the ultrafast Garrett transform fault near 13°28′S in the Pacific. Earth Planet. Sci. Lett. 108, 259–275.

Hildreth, W., Moorbath, S., 1988. Crustal contributions to arc magmatism in the Andes of Central Chile. Contrib. Mineral. Petrol. 98, 455–489.

Hyndman, R.D., Peacock, S.M., 2003. Serpentinization of the forearc mantle. Earth Planet. Sci. Lett. 212, 417–432.

Isacks, B.L., 1988. Uplift of the central Andean plateau and bending of the Bolivian orocline. J. Geophys. Res., Solid Earth (1978–2012) 93, 3211–3231.

Ishikawa, T., Nakamura, E., 1993. Boron isotope systematics of marine sediments. Earth Planet. Sci. Lett. 117, 567–580.

Ishikawa, T., Tera, F., 1997. Source, composition and distribution of the fluid in the Kurile mantle wedge: constraints from across-arc variations of B/Nb and B isotopes. Earth Planet. Sci. Lett. 152, 123–138.

Ishikawa, T., Tera, F., 1999. Two isotopically distinct fluid components involved in the Mariana arc: evidence from Nb/B ratios and B, Sr, Nd, and Pb isotope systematics. Geology 27, 83–86.

Ishikawa, T., Tera, F., Nakazawa, T., 2001. Boron isotope and trace element systematics of the three volcanic zones in the Kamchatka arc. Geochim. Cosmochim. Acta 65, 4523–4537.

Iyer, K., Rüpke, L.H., Morgan, J.P., 2010. Feedbacks between mantle hydration and hydrothermal convection at ocean spreading centers. Earth Planet. Sci. Lett. 296, 34–44.

James, D.E., 1982. A combined O, Sr, Nd, and Pb isotopic and trace element study of crustal contamination in central Andean lavas, I: local geochemical variations. Earth Planet. Sci. Lett. 57, 47–62.

Jarvis, A., Reuter, H.I., Nelson, A., Guevara, E., 2008. Hole-filled SRTM for the globe Version 4. Available from the CGIAR-CSI SRTM 90m Database.

Jones, R.E., 2014. Subduction zone processes and continental crust formation in the southern Central Andes: insights from geochemistry and geochronology. School of GeoSciences, The University of Edinburgh, Edinburgh.

Jordan, T., Allmendinger, R., Damanti, J., Drake, R., 1993. Chronology of motion in a complete thrust belt: the Precordillera, 30–31 S, Andes Mountains. J. Geol., 135–156.

Jordán, T.E., Isacks, B.L., Allmendinger, R.W., Brewer, J.A., Ramos, V.A., Ando, C.J., 1983. Andean tectonics related to geometry of subducted Nazca plate. Geol. Soc. Am. Bull. 94, 341–361.

Jordon, T.E., Burns, W.M., Veiga, R., Pángaro, F., Copeland, P., Kelley, S., Mpodozis, C., 2001. Extension and basin formation in the southern Andes caused by increased convergence rate: a mid-Cenozoic trigger for the Andes. Tectonics 20, 308–324.

Kasemann, S., Erzinger, J., Franz, G., 2000. Boron recycling in the continental crust of the central Andes from the Palaeozoic to Mesozoic, NW Argentina. Contrib. Mineral. Petrol. 140, 328–343.

Kay, S.M., Abbruzzi, J.M., 1996. Magmatic evidence for Neogene lithospheric evolution of the central Andean "flat slab" between 30°S and 32°S. Tectonophysics 259, 15–28.

Kay, S.M., Godoy, E., Kurtz, A., 2005. Episodic arc migration, crustal thickening, subduction erosion, and magmatism in the south-central Andes. Geol. Soc. Am. Bull. 117, 67–88.

Kay, S.M., Maksaev, V., Moscoso, R., Mpodozis, C., Nasi, C., 1987. Probing the evolving Andean lithosphere: Mid–Late Tertiary magmatism in Chile (29°–30°30′S) over the modern zone of subhorizontal subduction. J. Geophys. Res. 92, 6173–6189.

Kay, S.M., Mpodozis, C., 2002. Magmatism as a probe to the Neogene shallowing of the Nazca plate beneath the modern Chilean flat slab. J. South Am. Earth Sci. 15, 39–57.

Kay, S.M., Mpodozis, C., Ramos, V.A., Munizaga, F., 1991. Magma source variations for mid-late Tertiary magmatic rocks associated with a shallowing subduction zone and the thickening crust in the central Andes (28–33°S). In: Spec. Pap., Geological Society of America Bulletin, vol. 265, pp. 113–137.

Kilian, R., Behrmann, J.H., 2003. Geochemical constraints on the sources of Southern Chile Trench sediments and their recycling in arc magmas of the Southern Andes. J. Geol. Soc. 160, 57–70.

King, R.L., Bebout, G.E., Grove, M., Moriguti, T., Nakamura, E., 2007. Boron and lead isotope signatures of subduction-zone mélange formation: hybridization and fractionation along the slab–mantle interface beneath volcanic arcs. Chem. Geol. 239, 305–322.

Kopp, H., Flueh, E.R., Papenberg, C., Klaeschen, D., 2004. Seismic investigations of the O'Higgins Seamount Group and Juan Fernández Ridge: aseismic ridge emplacement and lithosphere hydration. Tectonics 23.

Leeman, W.P., Tonarini, S., Chan, L.H., Borg, L.E., 2004. Boron and lithium isotopic variations in a hot subduction zone—the southern Washington Cascades. Chem. Geol. 212, 101–124.

Litvak, V.D., Poma, S., 2010. Geochemistry of mafic Paleocene volcanic rocks in the Valle del Cura region: implications for the petrogenesis of primary mantle-derived melts over the Pampean flat-slab. J. South Am. Earth Sci. 29, 705–716.

Litvak, V.D., Poma, S., Kay, S.M., 2007. Paleogene and Neogene magmatism in the Valle del Cura region: new perspective on the evolution of the Pampean flat slab, San Juan province, Argentina. J. South Am. Earth Sci. 24, 117–137.

Lonsdale, P., 2005. Creation of the Cocos and Nazca plates by fission of the Farallon plate. Tectonophysics 404, 237–264.

Lucassen, F., Escayola, M., Romer, R.L., Viramonte, J., Koch, K., Franz, G., 2002. Isotopic composition of Late Mesozoic basic and ultrabasic rocks from the Andes (23–32 S)-implications for the Andean mantle. Contrib. Mineral. Petrol. 143, 336–349.

Maksaev, V., Moscoso, R., Mpodozis, C., Nasi, C., 1984. Las unidades volcánicas y plutónicas del Cenozoico superior en la Alta Cordilera del Norte Chico (29°–31°S): Geología, Alteración hidrotermal y Mineralización. Rev. Geol. Chile 11, 12–51.

Manea, V.C., Pérez-Gussinyé, M., Manea, M., 2012. Chilean flat slab subduction controlled by overriding plate thickness and trench rollback. Geology 40, 35–38.

Marot, M., Monfret, T., Pardo, M., Ranalli, G., Nolet, G., 2013. A double seismic zone in the subducting Juan Fernandez Ridge of the Nazca Plate (32°S), central Chile. J. Geophys. Res., Solid Earth 118, 3462–3475.

Marschall, H.R., Altherr, R., Kalt, A., Ludwig, T., 2008. Detrital, metamorphic and metasomatic tourmaline in high-pressure metasediments from Syros (Greece): intra-grain boron isotope patterns determined by secondary-ion mass spectrometry. Contrib. Mineral. Petrol. 155, 703–717.

Marschall, H.R., Schumacher, J.C., 2012. Arc magmas sourced from melange diapirs in subduction zones. Nat. Geosci. 5, 862–867.

McGeary, S., Nur, A., Ben-Avraham, Z., 1985. Spatial gaps in arc volcanism: the effect of collision or subduction of oceanic plateaus. Tectonophysics 119, 195–221.

Melson, W.G., Thompson, G., 1971. Petrology of a transform fault zone and adjacent ridge segments. Philos. Trans. R. Soc. Lond. Ser. A, Math. Phys. Sci. 268, 423–441.

Moran, A.E., Sisson, V.B., Leeman, W.P., 1992. Boron depletion during progressive metamorphism: implications for subduction processes. Earth Planet. Sci. Lett. 111, 331–349.

Oncken, O., Hindle, D., Kley, J., Elger, K., Victor, P., Schemmann, K., 2006. Deformation of the central Andean upper plate system—facts, fiction, and constraints for plateau models. In: The Andes. Springer, pp. 3–27.

Pabst, S., Zack, T., Savov, I.P., Ludwig, T., Rost, D., Tonarini, S., Vicenzi, E.P., 2012. The fate of subducted oceanic slabs in the shallow mantle: insights from boron isotopes and light element composition of metasomatized blueschists from the Mariana forearc. Lithos 132–133, 162–179.

Palmer, M., 1991. Boron-isotope systematics of Halmahera arc (Indonesia) lavas: evidence for involvement of the subducted slab. Geology 19, 215–217.

Parada, M.A., Rivano, S., Sepulveda, P., Herve, M., Herve, F., Puig, A., Munizaga, F., Brook, M., Pankhurst, R., Snelling, N., 1988. Mesozoic and Cenozoic plutonic development in the Andes of central Chile (30°30′–32°30′S). J. South Am. Earth Sci. 1, 249–260.
Pardo Casas, F., Molnar, P., 1987. Relative motion of the Nazca (Farallón) and South America plates since Late Cretaceous time. Tectonics 6, 233–248.
Peacock, S.A., 1990. Fluid processes in subduction zones. Science 248, 329–337.
Peacock, S.M., Hervig, R.L., 1999. Boron isotopic composition of subduction-zone metamorphic rocks. Chem. Geol. 160, 281–290.
Pilger, R.H., 1981. Plate reconstructions, aseismic ridges, and low angle subduction beneath the Andes. Geol. Soc. Am. Bull. 92, 448–456.
Pilger, R.H., 1984. Cenozoic plate kinematics, subduction and magmatism: South American Andes. J. Geol. Soc. Lond. 141, 793–802.
Ramos, V.A., Cristallini, E.O., Pérez, D.J., 2002. The Pampean flat-slab of the Central Andes. J. South Am. Earth Sci. 15, 59–78.
Ramos, V.A., Folguera, A., 2009. Andean flat-slab subduction through time. In: Geological Society, London, Special Publications, vol. 327, pp. 31–54.
Ramos, V.A., Kay, S.M., Page, R., Munizaga, F., 1989. La ignimbrita Vacas Heladas y el cese del volcanismo en el Valle del Cura, Provincia de San Juan. Rev. Asoc. Geol. Argent. 44, 336–352.
Ranero, C., Morgan, J.P., McIntosh, K., Reichert, C., 2003. Bending-related faulting and mantle serpentinization at the Middle America trench. Nature 425, 367–373.
Ranero, C.R., Sallarès, V., 2004. Geophysical evidence for hydration of the crust and mantle of the Nazca plate during bending at the north Chile trench. Geology 32, 549–552.
Reiners, P.W., Nelson, B.K., Ghiorso, M.S., 1995. Assimilation of felsic crust by basaltic magma: thermal limits and extents of crustal contamination of mantle-derived magmas. Geology 23, 563–566.
Rosner, M., Erzinger, J., Franz, G., Trumbull, R.B., 2003. Slab-derived boron isotope signatures in arc volcanic rocks from the Central Andes and evidence from boron isotope fractination during progressive slab dehydration. Geochem. Geophys. Geosyst. 4.
Rüpke, L.H., Morgan, J.P., Hort, M., Connolly, J.A.D., 2004. Serpentine and the subduction zone water cycle. Earth Planet. Sci. Lett. 223, 17–34.
Rutland, R.W.R., 1971. Andean orogeny and ocean floor spreading. Nature 233, 252–255.
Ryan, J.G., Chauvel, C., 2014. 3.13—the subduction-zone filter and the impact of recycled materials on the evolution of the mantle. In: Holland, H.D., Turekian, K.K. (Eds.), second edition. Treatise on Geochemistry. Elsevier, Oxford, pp. 479–508.
Ryan, J.G., Leeman, W.P., Morris, J.D., Langmuir, C.H., 1996. The boron systematics of intraplate lavas: implications for crust and mantle evolution. Geochim. Cosmochim. Acta 60, 415–422.
Ryan, J.G., Morris, J.D., Tera, F., Leeman, W.P., Tsuetkov, A., 1995. Cross-arc geochemical variations in the Kurile arc as a function of slab depth. Science 270, 625–627.
Savov, I.P., Ryan, J.G., D'Antonio, M., Fryer, P., 2007. Shallow slab fluid release across and along the Mariana arc-basin system: insights from geochemistry of serpentinized peridotites from the Mariana fore arc. J. Geophys. Res., Solid Earth 112, B09205.
Schiano, P., 2003. Primitive mantle magmas recorded as silicate melt inclusions in igneous minerals. Earth-Sci. Rev. 63, 121–144.
Schmitt, A.K., Kasemann, S., Meixner, A., Rhede, D., 2002. Boron in central Andean ignimbrites: implications for crustal boron cycles in active continental margin. Chem. Geol. 183, 333–347.
Scholl, D.W., Christensen, M.N., Von Huene, R., Marlow, M.S., 1970. Peru–Chile trench sediments and sea-floor spreading. Geol. Soc. Am. Bull. 81, 1339–1360.
Silver, P.G., Russo, R.M., Lithgow-Bertelloni, C., 1998. Coupling of South American and African plate motion and plate deformation. Science 279, 60–63.
Smith, H.J., Leeman, W.P., Davidson, J., Spivack, A.J., 1997. The B isotopic composition of arc lavas from Martinique, Lesser Antilles. Earth Planet. Sci. Lett. 146, 303–314.
Smith, H.J., Spivack, A.J., Staudigel, H., Hart, S.R., 1995. The boron isotopic composition of altered oceanic crust. Chem. Geol. 126, 119–135.
Sobolev, A.V., 1996. Melt inclusions in minerals as a source of principle petrological information. Petrology 4, 209–220.
Somoza, R., 1998. Updated azca (Farallon)—South America relative motions during the last 40 My: implications for mountain building in the central Andean region. J. South Am. Earth Sci. 11, 211–215.
Somoza, R., Ghidella, M.E., 2012. Late Cretaceous to recent plate motions in western South America revisited. Earth Planet. Sci. Lett. 331–332, 152–163.
Spandler, C., Pirard, C., 2013. Element recycling from subducting slabs to arc crust: a review. Lithos 170–171, 208–223.
Spivack, A.J., Edmond, J.M., 1987. Boron isotope exchenge between seawater and the oceanic crust. Geochim. Cosmochim. Acta 51, 1033–1043.
Stern, C.R., 1991. Role of subduction erosion in the generation of Andean magmas. Geology 19, 78–81.
Stern, C.R., 2004. Active Andean volcanism: its geologic and tectonic setting. Rev. Geol. Chile 31, 161–206.
Straub, S.M., Layne, G.D., 2002. The systematics of boron isotopes in Izu arc front volcanic rocks. Earth Planet. Sci. Lett. 198, 25–39.
Syracuse, E.M., van Keken, P.E., Abers, G.A., 2010. The global range of subduction zone thermal models. Phys. Earth Planet. Inter. 183, 73–90.
Thornburg, T.M., Kulm, L.D., 1987a. Sedimentation in the Chile Trench: depositional morphologies, lithofacies, and stratigraphy. Geol. Soc. Am. Bull. 98, 33–52.
Thornburg, T.M., Kulm, L.D., 1987b. Sedimentation in the Chile Trench: petrofacies and provenance. J. Sediment. Res. 57, 55–74.
Tonarini, S., Leeman, W.P., Leat, P.T., 2011. Subduction erosion of forearc mantle wedge implicated in the genesis of the South Sandwich Island (SSI) arc: evidence from boron isotope systematics. Earth Planet. Sci. Lett. 301, 275–284.
Trumbull, R.B., Riller, U., Oncken, O., Scheuber, E., Munier, K., Hongn, F., 2006. The time–space distribution of Cenozoic Volcanism in the South–Central Andes: a new data compilation and some tectonic implications. In: Oncken, O., Chong, G., Franz, G., Giese, P., Götze, H.-J., Ramos, V.A., Strecker, M.R., Wigger, P. (Eds.), The Andes – Active Subduction Orogeny. Springer-Verlag, pp. 29–43.
Ulmer, P., Trommsdorff, V., 1995. Serpentine stability to mantle depths and subduction-related magmatism. Science 268, 858–861.
van Hunen, J., Van Den Berg, A.P., Vlaar, N.J., 2002. On the role of subducting oceanic plateaus in the development of shallow flat subduction. Tectonophysics 352, 317–333.
van Keken, P.E., Hacker, B.R., Syracuse, E.M., Abers, G.A., 2011. Subduction factory: 4. Depth-dependent flux of H_2O from subducting slabs worldwide. J. Geophys. Res., Solid Earth (1978–2012), 116.
Vils, F., Müntener, O., Kalt, A., Ludwig, T., 2011. Implications of the serpentine phase transition on the behaviour of beryllium and lithium–boron of subducted ultramafic rocks. Geochim. Cosmochim. Acta 75, 1249–1271.
Vils, F., Tonarini, S., Kalt, A., Seitz, H.-M., 2009. Boron, lithium and strontium isotopes as tracers of seawater–serpentinite interaction at Mid-Atlantic ridge, ODP Leg 209. Earth Planet. Sci. Lett. 286, 414–425.
Von Huene, R., Scholl, D.W., 1991. Observations at convergent margins concerning sediment subduction, subduction erosion, and the growth of continental crust. Rev. Geophys. 29.
Winocur, D., Litvak, V., Ramos, V., 2014. Magmatic and tectonic evolution of the Oligocene Valle del Cura basin, main Andes of Argentina and Chile: evidence for generalized extension. In: Geological Society, London, Special Publications, vol. 399, p. 392. SP399.
Wittenbrink, J., Lehmann, B., Wiedenbeck, M., Wallianos, A., Dietrich, A., Palacios, C., 2009. Boron isotope composition of melt inclusions from porphyry systems of the Central Andes: a reconnaissance study. Terra Nova 21, 111–118.
Workman, R.K., Hart, S.R., 2005. Major and trace element composition of the depleted MORB mantle (DMM). Earth Planet. Sci. Lett. 231, 53–72.
Wunder, B., Wirth, R., Gottschalk, M., 2001. Antigorite pressure and temperature dependence of polysomatism and water content. Eur. J. Mineral. 13, 485–496.
Yamaoka, K., Ishikawa, T., Matsubaya, O., Ishiyama, D., Nagaishi, K., Hiroyasu, Y., Chiba, H., Kawahata, H., 2012. Boron and oxygen isotope systematics for a complete section of oceanic crustal rocks in the Oman ophiolite. Geochim. Cosmochim. Acta 84, 543–559.
Yamaoka, K., Matsukura, S., Ishikawa, T., Kawahata, H., 2011. Boron contents and isotope compositions of oceanic crusts from the Oman and Troodos ophiolites. In: AGU Fall Meeting Abstracts, p. 1484.
Yañez, G.A., Cembrano, J., Pardo, M., Ranero, C.R., Selles, D., 2002. The Challenger – Juan Fernández – Maipo major tectonic transition of the Nazca – Andean subduction system at 33–34°S: geodynamic evidence and implications. J. South Am. Earth Sci. 15, 28–38.
Yañez, G.A., Ranero, C.R., von Huene, R., Díaz, J., 2001. Magnetic anomaly interpretation across the southern central Andes (32°–34°S): the role of the Juan Fernández Ridge in the late Tertiary evolution of the margin. J. Geophys. Res. 106, 6325–6345.
You, C.F., Castillo, P.R., Gieskes, J.M., Chan, L.H., Spivack, A.J., 1996. Trace element behavior in hydrothermal experiments: implications for fluid processes at shallow depths in subduction zones. Earth Planet. Sci. Lett. 140, 41–52.
You, C.F., Spivack, A.J., Gieskes, J.M., Rosenbauer, R., Bischoff, J.L., 1995. Experimental study of boron geochemistry: implications for fluid processes in subduction zones. Geochim. Cosmochim. Acta 59, 2435–2442.